



Published in final edited form as:

Exp Neurol. 2010 November ; 226(1): 242–253. doi:10.1016/j.expneurol.2010.08.036.

Impaired immune responses following spinal cord injury lead to reduced ability to control viral infection

Katherine S. Held^a, Oswald Steward^{a,b}, Caroline Blanc^c, and Thomas E. Lane^{c,d,*}

^aReeve-Irvine Research Center and Department of Anatomy and Neurobiology, University of California, Irvine School of Medicine, 92697-4265, USA

^bDepartment of Neurosurgery, University of California, Irvine, School of Medicine, 92697-4292, USA

^cDepartment of Molecular Biology and Biochemistry, University of California, Irvine, 92697-3900, USA

^dInstitute for Immunology and Sue and Bill Gross Stem Cell Center, University of California, Irvine, 92697-3900, USA

Abstract

Spinal cord injuries disrupt central autonomic pathways that regulate immune function, and increasing evidence suggests that this may cause deficiencies in immune responses in people with spinal cord injuries. Here we analyze the consequences of spinal cord injury (SCI) on immune responses following experimental viral infection of mice. Female C57BL/6 mice received complete crush injuries at either thoracic level 3 (T3) or 9 (T9), and 1 week post-injury, injured mice and un-injured controls were infected with different dosages of mouse hepatitis virus (MHV, a positive-strand RNA virus). Following MHV infection, T3- and T9-injured mice exhibited increased mortality in comparison to un-injured and laminectomy controls. Infection at all dosages resulted in significantly higher viral titer in both T3- and T9-injured mice compared to un-injured controls. Investigation of anti-viral immune responses revealed impairment of cellular infiltration and effector functions in mice with SCI. Specifically, cell-mediated responses were diminished in T3-injured mice, as seen by reduction in virus-specific CD4⁺ T lymphocyte proliferation and IFN- γ production and decreased numbers of activated antigen presenting cells compared to infected un-injured mice. Collectively, these data indicate that the inability to control viral replication following SCI is not level dependent and that increased susceptibility to infection is due to suppression of both innate and adaptive immune responses.

Keywords

Spinal cord injury; Virus; Infection; Spleen; Immunosuppression; Immunity; Autonomic

*Corresponding author. Department of Molecular Biology & Biochemistry, 3205 McGaugh Hall, University of California, Irvine, Irvine, CA 92697-3900, USA. Fax: +1 949 825 8551. tlane@uci.edu (T.E. Lane).

The authors of this manuscript have no conflict of interest.

Introduction

People with spinal cord injury (SCI) exhibit increased risk of infection; indeed, complications from infection are the leading cause of re-hospitalization and death in the post-acute phase following SCI (Cardenas et al., 2004; Soden et al., 2000). Understanding the mechanisms underlying this increased susceptibility could lead to therapeutic treatments to improve the lives of many with neurological disorders. One possible explanation of increased susceptibility to infection following SCI is a disruption of immune responses due to interruption of neural pathways that regulate immune effector functions required to control and eliminate the invading pathogen. One important route of communication is via central autonomic pathways that descend via the spinal cord. These regulate the output of preganglionic sympathetic axons that innervate lymphoid organs including the spleen (Mignini et al., 2003). Injury to the spinal cord at cervical or high thoracic levels can damage these pathways, which would disrupt descending control of preganglionic sympathetic neurons below the injury; as a result, their output to peripheral lymphoid tissues would not be regulated by supraspinal control. Similarly, injury at mid-thoracic levels would damage some preganglionic sympathetic neurons directly.

Clinical studies reveal that people with SCI have muted neutrophil phagocytosis, natural killer (NK) cell cytotoxicity and T lymphocyte activation compared to control subjects, indicating suppression of innate and adaptive immune responses following SCI. (Campagnolo et al., 1997; Campagnolo et al., 2008; Cruse et al., 2000a). Furthermore, the nature of the immune deficiencies following SCI may depend on the level of the injury, presumably because decentralized sympathetic outflow occurs following injury at mid-thoracic or higher levels (Cano et al., 2001; Teasell et al., 2000). While reduced phagocytosis is observed in tetraplegics compared to paraplegics, alterations in NK and T lymphocyte cytotoxic activity are not level dependent (Campagnolo et al., 2008; Iversen et al., 2000). In addition, experimental SCI models have shown level-dependent impairment of B cell functions (Lucin et al., 2007). Studies by Popovich and colleagues reveal alterations in B lymphocyte and humoral immune responses in mice following injuries at thoracic level (T3), which would disrupt descending autonomic control of the spleen, but not following injuries at T9. Although the consequences of sympathetic decentralization to immunity are not fully elucidated, these observations suggest that SCI can result in immune suppression, which could impair ability to mount a protective immune response following infection.

Thus far, neural-immune suppression following SCI has been characterized by assessing acquired immunity to a specific challenge with innocuous antigen. However, for spinal cord injured people, the key issue is response to infectious challenge. Here, we describe an animal model of this phenomenon. We evaluated survival and antiviral immune responses in mice with SCI at T3 or T9 following infection with mouse hepatitis virus (MHV). Intraperitoneal infection of immunocompetent mice with the hepatotropic A59 strain of MHV results in an acute hepatitis. Anti-viral host defense to MHV infection involves a robust Type-1 T helper cell (Th1)-mediated immune response, and virus-specific T lymphocytes generated within the spleen that migrate into the liver and clear virus through secretion of the anti-viral cytokine IFN- γ as well as cytotoxic activity (Schijns et al., 1998; Walsh et al., 2007; Wijburg et al., 1996). We show here that mice with high and low thoracic

spinal cord injuries have increased viral load and increased mortality in comparison to uninjured mice. Thus increased sensitivity to viral infection is not injury-level dependent. Furthermore, high-level injury results in impaired innate and virus-specific immune responses. These results reveal a murine model for increased susceptibility to viral infection as a consequence of SCI.

Materials and methods

Virus and mice

Mouse hepatitis virus (MHV; a positive-strand RNA virus that is a member of the *Coronaviridae* family) strain A59 was used in all experiments described. MHV-A59 replicates within the liver, without central nervous system infection, following intraperitoneal (i.p.) injection of C57BL/6 mice (Navas et al., 2001). Age-matched 5- to 7-week-old female C57BL/6 mice (H-2^b background) were purchased from the National Cancer Institute, Bethesda, Maryland, and used for all experiments. Mice infected with virus received 100 μ l i.p. sterile saline suspension of MHV at 5×10^5 PFU, 1×10^4 PFU or 5×10^2 PFU, while uninfected control mice received 100 μ l sterile saline alone. Infections occurred 1 or 4 weeks following spinal cord injury. Animals were euthanized at defined time points, perfused with 20 ml sterile $1 \times$ PBS, and tissues removed for analysis. All procedures were approved by the Institutional Animal Care and Use Committee of the University of California Irvine.

Spinal cord injury

Mice were initially anesthetized with Avertin (0.5 ml/20 g); when supplemental anesthesia was required, one-fourth of the original dose was given. Body temperature was maintained by placing mice on a water-circulating jacketed heating pad at 37 ± 0.5 °C. The skin over the upper thoracic area was shaved and cleaned with a Betadine solution. Using aseptic techniques, the skin was incised and connective and muscle tissues were bluntly dissected to expose the third vertebral body (T3) or the ninth (T9). A laminectomy was performed at T3 or T9 to expose the dorsal spinal cord. Sham-injured animals received a laminectomy, but no SCI. Un-injured mice did not undergo any surgery, but were anesthetized. Complete crush injuries were performed using forceps (Dumont #5) placed on either side of exposed spinal cord following laminectomy. The points of the forceps were then brought together, held for 1 s, and released. A complete crush injury results in loss of motor function caudal to the injury site. After injury, the muscles and skin were sutured separately and mice given subcutaneous injections of lactated Ringer's solution (1 ml/20 g) for hydration, Buprenex (Buprenorphine, 0.05 mg/kg) for analgesia, and Baytril (Enrofloxacin, 2.5 mg/kg) for prophylaxis against urinary tract infections. Mice were placed in cages with Alpha-Dri bedding (Newco Distributors Inc.), warmed directly on water-jacketed heating pads at 37 °C, until recovered from anesthesia. Thereafter, half of each cage was placed on heating jacket for up to 3 days post-surgery, until coat quality improved and mobility around the cage resumed: Non-surgery and sham-injured mice recovered within the first 24 h, while T3- and T9-injured mice recovered within 36 h. Post-operative care involved daily treatments of lactated Ringer's solution and Baytril for the first 6 days post-surgery, and daily Buprenex treatments

for the first 3 days post-surgery. Post-operative care of injured mice also included manual bladder expression 2×/day for the duration of experiments.

Viral titer

Liver lobes were removed at defined time points, weighed, and homogenized. Tenfold serial dilutions of liver neat were tittered by plaque assay on a mouse DBT astrocytoma cell line (Hirano et al., 1978; Lane et al., 2000).

Mononuclear cell isolation and flow cytometric analysis

Mononuclear cells were obtained from whole spleen and liver at defined times using previously described methods (Stiles et al., 2006; Walsh et al., 2007). Immunophenotyping of cells was performed using the following DB Pharmingen (San Diego, CA) antibodies: fluorescein isothiocyanate (FITC)-conjugated CD45R/B220, allophycoerythrin (APC)-conjugated rat anti-mouse CD4 and CD8, APC-conjugated mouse anti-mouse NK1.1, phycoerythrin (PE)-conjugated Golden Syrian hamster anti-mouse CD3e, FITC-conjugated rat anti-mouse CD11b, PE-conjugated rat anti-mouse CD86, and PE-conjugated rat anti-mouse I/A-I/E (MHC II) (Held et al., 2008; Trifilo et al., 2004). In all cases, isotype-matched control antibodies were used. Virus-specific CD4⁺ and CD8⁺ T cells recognizing their respective immunodominant epitope between amino acids 133 and 147 of the membrane (M) glycoprotein (M133–147) and surface (S) glycoprotein (S598–605) were determined by intracellular IFN- γ staining using previously described methods (Bergmann et al., 1996; Xue et al., 1995). In brief, 1×10^6 total cells were stimulated *ex vivo* with a 5 μ M final concentration of viral peptides or non-specific Ovalbumin, OVA, for 6 h at 37 °C, 5% CO₂ in complete media containing Golgi stop (Cytofix/Cytoperm kit; Pharmingen), after which cells were washed and Fc receptor blocked with 1 \times PBS containing 10% FBS and a 1:200 dilution of rat anti-mouse CD16/32 antibody (Pharmingen). Cells were then stained for surface antigens using APC-conjugated rat antimouse CD4 and CD8 (Pharmingen), according to the viral peptide stimulation condition, for 45 min at 4 °C. Cells were fixed and permeabilized using a Cytofix/Cytoperm kit and stained for intracellular IFN- γ using phycoerythrin PE-conjugated anti-IFN- γ (1:50; XMG1.2, Pharmingen) for 45 min at 4 °C. Cells were washed and flow cytometry was performed using a FACStar flow cytometer (Becton Dickinson, Mountain View, CA). FlowJo software (Tree Star, Inc.) was used for data analysis, and approximately 5×10^4 live cell events were assessed from each sample to determine the frequency of stained populations. Frequency data are presented as the percentage of positive cells within the gated population. Total cell numbers were calculated by multiplying these values by the total number of live cells isolated and quantified using trypan blue-hemocytometer method.

ELISA

Splenocytes were isolated from mice at day 5 post-infection, and cultured for 60 h at 37 °C, 5% CO₂ in complete media under antigen stimulation. 2.5×10^6 total cells/well were plated in 24 well plate, and each well stimulated with 5 μ M final peptide concentration of CD4⁺ T cell immunodominant epitope M133–147, CD8⁺ T cell subdominant epitope S598–605 (Biosynthesis), or non-specific Ovalbumin, OVA, (American Peptide Co.) control.

Supernatants were harvested and IFN- γ , IL-10, and IL-17 were quantified using the Mouse DuoSet ELISA (R&D Systems, Inc.).

In vitro T cell proliferation assay

Splenocytes were isolated from mice at day 5 post-infection and labeled with the fluorescent dye, carboxyfluorescein diacetate succinimidyl ester (CFSE), (Molecular Probes) at a 2.5 μ M final concentration. 1×10^6 total cells/well were stimulated with a 5 μ M final peptide concentration of CD4⁺ T cell immunodominant epitope M133–147, CD8⁺ T cell subdominant epitope S598–605, or non-specific OVA control, and cultured for 60 h at 37 °C, 5% CO₂ in complete media. Cells were then washed and Fc receptor blocked with 1 \times PBS containing 10% FBS and a 1:200 dilution of rat anti-mouse CD16/32 antibody (Pharmingen). Next, cells were stained for surface antigens using APC-conjugated rat anti-mouse CD4 and CD8 (Pharmingen), according to the viral peptide stimulation condition, for 45 min at 4 °C. Cells were analyzed and data assessed as described above.

Statistical analysis

Differences in viral titer data between SCI and un-injured infected groups were assessed by Mann–Whitney test. Comparisons between injured and un-injured groups before and after MHV infection were by one-way ANOVA. Bonferroni corrections were used for multiple comparisons. Analyses were done using JMP 8 software (SAS Institute, Inc.) and *p* values of 0.05 were considered significant.

Results

SCI leads to increased mortality and higher viral titer following viral infection compared to un-injured infected mice

Infection of un-injured C57BL/6 female mice with 5×10^5 PFU MHV leads to acute hepatitis infection, but all mice survive and recover and this is associated with clearance of virus from the liver to below levels detectable by plaque assay (~ 200 PFU/g tissue) (Eriksson et al., 2008; Navas et al., 2001). In contrast, all mice that received 5×10^5 PFU of MHV 1 week following a complete bilateral crush SCI at thoracic level-T3 died by 6 days post-infection (p.i.) (Fig. 1A). Similarly, infection of T9-injured mice also resulted in 100% mortality by day 7 p.i. A striking increase in mortality was also seen following infection of T3-injured mice with 1×10^4 and even 5×10^2 PFU, although with both infectious doses some mice did survive (22% and 40%, respectively) (Fig. 1A). Infection of un-injured mice with either 1×10^4 or 5×10^2 PFU of virus resulted in 100% survival. All 10 mice that received a spinal cord injury but no viral injection survived. Importantly, increased mortality was not seen following the surgical laminectomy-control, indicating that the increased mortality was due to the SCI and not to the general surgical trauma.

One explanation for increased mortality is an impaired ability to control viral replication within the liver over the course of the infection. In un-injured C57Bl/6 mice infected with MHV, viral titers increase over the first few days after infection as virus replicates and spreads within the liver, and then decrease as virus-specific T lymphocytes expand and migrate into the liver to eliminate virus. Control of viral replication was impaired in mice

with SCI at levels T3 and T9. Comparisons of viral liver titers at 1 week post-SCI in mice that were infected with various dosages of virus revealed significantly ($p < 0.05$) greater viral load in injured mice vs. un-injured controls with similar titers present within the livers of T3- and T9-injured animals up to day 5 p.i. (Fig. 1B). By day 7 p.i. with 5×10^2 PFU, virus was reduced to below levels of detection in 83% (5 out of 6 mice) of un-injured mice and 100% (3 mice) of T9-injured mice cleared infection; yet only 25% (1 out of 4 mice) of T3-injured mice were able to clear virus, thus titers remained significantly high (Fig. 1B). Comparison of viral titers when mice were infected at 4 weeks post-SCI also revealed significantly higher viral load in T3- and T9-injured mice indicating that impaired control of viral replication is not restricted to early stages following injury ($p < 0.002$) (Fig. 1C). In addition, T3-injured mice showed significantly higher viral titer compared to T9-injured mice following infection at 4 weeks post-SCI ($p < 0.003$) (Fig. 1C). Thus, differences in the ability to control viral infection between T9-injured mice and T3-injured mice become apparent at day 7 p.i. upon infection with lower viral dosage (Fig. 1B) as well as following infection of mice at 4 weeks post-SCI (Fig. 1C). These findings suggest viral dosage and time of infection relative to SCI may differentially influence viral titer in T3- and T9-injured mice. Nonetheless, both T3- and T9-injured mice showed increased sensitivity to viral infection compared to un-injured mice at all dosages tested, which correlates to increased mortality following infection. Collectively, these findings indicate that SCI leads to a functional impairment of immune-mediated control of viral replication and this is independent of the level of injury following infection at 1 week post-SCI.

Alterations within the spleen following T3 and T9 injury

Following SCI, humans and experimental animals have aberrant numbers of circulating lymphocytes including natural killer (NK) cells and T and B cells (Campagnolo et al., 2008; Riegger et al., 2007). In addition, experimental injury at T3 in mice results in reduced spleen size compared to un-injured control mice at day 3 post-injury (Lucin et al., 2007). Here, assessments of spleen size revealed that by 1 week post-injury, spleen weight of T3-injured mice decreased approximately 25% in comparison to un-injured control mice and remained significantly ($p < 0.001$) decreased at 4 weeks post-injury (Fig. 2A). Following T9-injury, there was no dramatic reduction in spleen size compared to un-injured mice at 1 week post-injury, yet by 4 weeks following injury the spleens weighed significantly less ($p < 0.001$) compared to un-injured mice. (Fig. 2A). The average spleen weight of an un-injured C57BL/6 female mouse at 5–8 weeks of age is 70–89 mg (Lucin et al., 2007; Schmid et al., 1967) and increases with age, therefore, at 4 weeks post-SCI, injured mice had significantly smaller spleens compared to un-injured mice after an additional 3 weeks.

Injury-induced changes in the spleen were further evaluated by immunophenotyping B and T lymphocytes at 1 week post-SCI (Figs. 2B–D). While the frequency and number of B lymphocytes (CD45R/B220⁺ cells) in T9-injured mice were similar to un-injured mice (Fig. 2B, dot plots and graph), the frequency and number of B lymphocytes were reduced in T3-injured mice, and a difference in the number of cells was significant in comparison to un-injured control ($p < 0.002$) (Fig. 2B, dot plots and graph). The frequency of CD8⁺ T cells was increased in both T3- and T9-injured mice, but differences were statistically significant in comparison to control ($p < 0.004$) only in T3-injured mice (Fig. 2C, dot plots). However,

there were no differences in the numbers of CD8⁺ T cells between all groups (Fig. 2C, graph). T3-injured mice showed a significant increase in the frequency of CD4⁺ T cells compared to un-injured (*p = 0.006) and T9-injured (***p = 0.001) mice (Fig. 2D, dot plots); however the numbers of CD4⁺ T cells was similar between all groups (Fig. 2D, graph). These data show the SCI does not alter the number of T lymphocytes in the spleen at 1 week post-SCI, however, B lymphocytes were significantly reduced in T3-injured mice compared to un-injured controls, indicating this particular cellular reduction may contribute to the decrease in spleen size. B lymphocytes are not required for MHV clearance from the liver (Matthews et al., 2001), therefore, based upon similar deficiencies in controlling viral replication in both T3- and T9-injured mice, we focused our attention on T3-injury to define specific immunological parameters that are affected following infection.

Lymphocyte responses in T3-injured mice following MHV infection

At 1 week and 4 weeks post-SCI, we infected T3-injured and uninjured mice with 1×10^4 PFU MHV to assess how SCI influenced immune cell responses within the spleen. Within the first week following MHV infection, T cell responses are initiated in lymphatic tissue, including the spleen, by activated antigen presenting cells (APCs). The influx of leukocytes, including APCs, to the spleen and expansion of effector T cells contribute to spleen enlargement, as was observed in both T3-injured and un-injured infected mice at day 5 post-infection (Fig. 3A). However, spleen sizes were significantly smaller in mice with T3-SCI at both 1 and 4 weeks post-injury (p = 0.03) (Fig. 3A). Relative to spleen weight prior to infection (Fig. 2A), T3-injured and un-injured mice share similar percent enlargement (~50% change in weight), suggesting T3-injured mice are able to respond to viral infection. We continued our studies with mice infected with 1×10^4 PFU MHV at 1 week post-SCI to assess T lymphocyte responses within the spleen. The frequency of CD8⁺ T cells within the spleens of T3-SCI mice was significantly (p = 0.002) higher compared to un-injured mice (Fig. 3B, first panel), yet there was no difference in overall numbers of CD8⁺ T cells within the spleens of injured mice infected with virus compared to virally-infected un-injured mice (Fig. 3B, second panel). In contrast, the frequency of CD4⁺ T cells in experimental groups was similar (Fig. 3C, first panel) while the total numbers of CD4⁺ T cells were significantly (p = 0.04) reduced in injured mice infected with MHV when compared to infected un-injured mice (Fig. 3C, second panel). Statements on statistical significance pertain to the combined data from the two experiments. The numbers of animals were too low in each individual experiment for meaningful statistical analyses, but similar trends were seen.

To determine whether generation of virus-specific T lymphocytes was affected by SCI, we measured intracellular IFN- γ staining following *ex vivo* stimulation with virus-specific peptides S598–605 and M133–147 that correspond to defined CD8⁺ and CD4⁺ T cell epitopes, respectively (Castro and Perlman, 1995; Xue et al., 1995). This assay revealed similar numbers of virus-specific CD8⁺ T cells (Fig. 3B, right-hand panel), but significantly (p = 0.003) decreased numbers of virus-specific CD4⁺ T lymphocytes in spinal cord injured mice (Fig. 3C, right-hand panel). Flow cytometric analysis for antigen presenting cells (APCs) *e.g.* macrophages and dendritic cells, and the level of activation was determined using CD11b and CD86 surface antigen markers. While the frequency of APCs (CD11b⁺ cells) was significantly increased in T3-injured mice (p = 0.04) (Fig. 3D, first panel), the

level of APCs activation, as determined by dual-positive CD11b⁺ CD86⁺ surface antigens, was significantly reduced compared to un-injured mice ($p < 0.01$) (Fig. 3D, second panel). Together, these findings indicate that viral infection of T3-injured mice results in reduced spleen size, reduced activation of APCs, fewer helper T cells, and diminished numbers of virus-specific CD4⁺ T cells.

Diminished proliferation and IFN- γ production by virus-specific CD4⁺ T cells isolated from the spleens of T3-injured mice

To determine the effects of T3 injury on T lymphocyte responses to MHV infection, we first evaluated proliferation of virus-specific T cells isolated from the spleens of experimental mice in response to stimulation with virus-specific peptides S598–605 and M133–147; the measure of proliferation was the loss of CFSE incorporation into replicating cells. CD8⁺ T cell proliferation following peptide stimulation did not differ in T3-injured vs. un-injured infected mice (Figs. 4A and B). In marked contrast, proliferation of M133–147-specific CD4⁺ T cells, indicated by the frequency and number (Figs. 4C and D), was reduced in T3-injured mice compared to un-injured controls, with significantly ($p < 0.007$) decreased numbers in injured mice (Fig. 4D). Corresponding to diminished proliferation of M133–147-specific CD4⁺ T cell responses in injured mice, IFN- γ production by splenocytes following M133–147 peptide stimulation was also significantly ($p < 0.001$) reduced in infected T3-injured mice compared to infected un-injured mice (Fig. 4F). In contrast, IFN- γ production by virus-specific CD8⁺ T cells did not significantly differ in injured vs. un-injured mice infected with virus (Fig. 4E). IFN- γ production by uninfected injured and un-injured mice was minimal, yet similar between experimental groups (Figs. 4E and F). In addition, there were no differences in production of immunomodulating cytokines such as IL-10 or IL-17 between injured vs. un-injured mice (not shown).

NK and NK T cells infiltration into livers of injured mice infected with virus is not affected

We have previously demonstrated an important role for NK cells/NK T cells in controlling MHV replication within the liver (Muse et al., 2008; Walsh et al., 2007; Walsh et al., 2008). Increased susceptibility to MHV infection following SCI was not the result on impaired accumulation of either population as there were similar numbers of NK1.1⁺ cells ($1.4 \times 10^6 \pm 1.3 \times 10^5$, $n = 9$) in infected un-injured mice compared to infected T3-injured mice ($1.3 \times 10^6 \pm 1.4 \times 10^5$, $n = 9$) as determined by FACS staining of liver single cell suspensions at day 5 post-infection with 1×10^4 PFU of virus. Similarly, there were no differences in infiltration of NK T cells (NK1.1⁺CD3⁺) within the livers of MHV-infected un-injured mice ($2.7 \times 10^5 \pm 3.5 \times 10^4$, $n = 9$) compared to injured mice ($2.4 \times 10^5 \pm 2.1 \times 10^4$, $n = 9$). In addition, there were no differences in either NK or NK T cells within the livers of experimental mice prior to infection indicating that injury did not modulate trafficking of these lymphocyte populations. Importantly, these findings argue that inability to control viral replication within the liver following T3-SCI is not the result of impaired migration of either NK cells or NK T cells.

Macrophage activation is reduced in injured mice infected with virus

We next assessed whether macrophage infiltration into the liver was impaired in injured mice. Surface staining for CD11b revealed comparable total numbers of macrophages within

the livers of T3-injured and un-injured mice at day 5 p.i. (Fig. 5A). However, the frequency of dual-positive CD11b^{hi} MHC class II⁺ cells within the livers of infected injured mice was significantly ($p = 0.0001$) reduced compared to infected un-injured mice (Fig. 5B). Also, quantification of overall numbers of CD11b^{hi}MHC class II⁺ dual-positive cells revealed a significant ($p = 0.003$) reduction in activated macrophages in injured mice following infection (Fig. 5C). The numbers of total and activated macrophages detected within the livers prior to infection was minimal, yet similar between T3-injured and un-injured uninfected mice (Figs. 5A and C). Thus, while migration and accumulation of macrophages within the livers of injured mice infected with virus were not affected as evidenced by CD11b staining, infiltrating macrophages exhibited a muted activation profile that may contribute to deficiencies in immune-mediated control of viral replication via impaired antigen presentation. These findings indicate that signals involved in macrophage recruitment are not impacted following SCI, yet activation of macrophages is negatively affected.

Diminished accumulation of virus-specific CD4⁺ T cells within the livers of T3-injured mice infected with virus

Generation and migration of virus-specific T cells is critical in controlling and eventually reducing viral titers below level of detection within infected tissues. Therefore, we next evaluated T cell infiltration into the livers of T3-injured mice prior to infection and at day 5 p.i. Included in Fig. 6 are representative dot plots from infected mice with the frequency of total CD8⁺ or CD4⁺ T cell populations represented within the lower gate, while the frequency of dual-positive IFN- γ ⁺ T cells is shown in the upper gate. Flow cytometric analysis revealed no differences in either the frequency or numbers of CD8⁺ T cells between infected experimental groups (Figs. 6A and C). In contrast, there was a significant ($p = 0.006$) reduction in both the frequency and numbers of CD4⁺ T cells (Figs. 6B and E) within the livers of injured mice infected with virus compared to un-injured infected mice. Infiltration of virus-specific T lymphocytes into the livers of mice was determined using intracellular IFN- γ staining following stimulation of cells with peptides corresponding to CD4⁺ and CD8⁺ T cell epitopes. The frequency and number of CD8⁺ T cells recognizing the S598–605 peptide did not differ between groups (Figs. 6A and D). In contrast, the frequency and number of virus-specific CD4⁺ T cells responding to the M133–147 peptide were significantly ($p = 0.01$) reduced in injured infected mice (Figs. 6B and F). The number of total T lymphocytes, including cells dual-positive for IFN- γ , was low in uninfected groups, yet similar between T3-injured and un-injured mice (Figs. 6C–F). Together, these data indicate that recruitment of CD4⁺ T cells into the livers of MHV-infected mice is impaired following T3-injury, and that this impairment correlates with the inability to control viral replication.

Discussion

The current study assessed how SCI impairs the ability to generate a protective immune response following viral infection. Immune suppression in people with SCI leads to increased morbidity and mortality (Cardenas et al., 2004), therefore it is surprising that there have been few studies documenting how SCI affects susceptibility following microbial

infection in animal models of injury. While impaired immunity has been studied following other forms of central nervous system (CNS)-injury, our results reveal a novel murine model for the increased susceptibility to infection that is seen in spinal cord injured people. In sum, our findings reveal that reduced activation of APCs within the spleen and liver following MHV infection correlates with impaired generation and effector function of virus-specific CD4⁺ T cells and this ultimately resulted in diminished ability to control viral replication. To our knowledge, this is the first report to unequivocally demonstrate that generation of an adaptive immune response to a viral pathogen is dramatically altered following SCI. Moreover, our findings indicate that the elevated susceptibility to viral infection is not dependent on the level of injury.

A potential cause of altered immune responses following SCI is a disruption of central autonomic pathways that regulate immune function, which descend from the brain to terminate on preganglionic sympathetic neurons. These preganglionic neurons project to postganglionic neurons that innervate primary and secondary lymphoid tissues (Bellinger et al., 1979; Cano et al., 2001; Lorton et al., 2005; Mignini et al., 2003). In this way, noradrenergic fibers modulate immune function primarily via β_2 adrenergic receptor (AR) signaling. A SCI that disrupts descending input to preganglionic sympathetic neurons would leave them unregulated by descending control, in much the same way that injuries disrupt descending control of segmental motor circuitry, causing hyper-reflexia and spasticity. Under normal circumstances, the sympathetic nervous system (SNS) and the hypothalamic-pituitary-adrenal (HPA) axis display a coordinated effort to modulate immune responses and maintain homeostasis (Downing and Miyan, 2000). However, following CNS injury, including stroke, traumatic brain injury and SCI, a CNS immune deficiency syndrome (CIDS) has been described as an over-compensatory anti-inflammation state resulting in depression of immune responses (Cruse et al., 1996; Meisel et al., 2005). Cumulative evidence supports that disruption of autonomic and neuroendocrine function is linked to increased incidence of infection in people with SCI (Cruse et al., 2000a,b; Klehmet et al., 2009; Meisel et al., 2005).

SCI-induced immune depression syndrome has been characterized by an acute decrease in leukocyte populations and function, which correlate with increased activities of SNS and HPA-axis, as determined by elevated levels of stress hormones (norepinephrine and cortisol, respectively) (Cruse et al., 1996; Cruse et al., 2000a,b; Meisel et al., 2005). Over time immune responses improve and stress hormone levels decrease (Cruse et al., 2000a,b; Riegger et al., 2007). Temporal evaluation of leukocytes in T8-injured rats revealed selective decrease in numbers of monocytes, dendritic cells, T and B lymphocytes, as well as expression of MHC II, all of which began to recover to control levels after 1 week post-SCI (Riegger et al., 2007). In addition, post-acute clinical assessment of subjects with SCI revealed the frequency of T lymphocytes is increased compared to control subjects (Campagnolo et al., 2008). Furthermore, rodent studies show increased SNS and HPA-axis activity at day 3 post-SCI, yet by 1 week post-high thoracic SCI injury, corticosterone levels are similar to un-injured controls (Lucin et al., 2007; MacNeil and Nance, 2001). Our splenocyte comparison of T3- and T9-injured mice to un-injured controls 1 week post-SCI may reflect recovery of deficits occurring at earlier time points and alterations in T lymphocyte frequency. However, B lymphocytes were significantly decreased in T3-injured

mice suggesting higher level injury results in selective suppression of this population. Previous studies support T3-injury-induced alteration in B lymphocytes, and have further shown cell survival and function are adversely affected by combinatory β_2 AR and glucocorticoid receptor signaling via high levels of stress hormones (Lucin et al., 2009). Current studies are addressing whether changes in the influx from primary lymphatic tissue and maturation of B lymphocytes in the spleen also contribute to these level-dependent changes.

Previous studies have shown that innate and adaptive immune responses are diminished following SCI. The development of adaptive immunity via cellular adhesion molecule signaling, as well as the proliferation of T lymphocytes in response mitogen stimulation were found to be reduced in human and animal studies (Campagnolo et al., 2008; Cruse et al., 2000a,b). The deregulation of autonomic and neuroendocrine influence on immune function can potentially lead to other forms of suppression following SCI. Interestingly, β_2 AR are expressed on Th1-associated CD4⁺ T cells and not Th2, providing specificity in catecholamine-immune regulation (Sanders et al., 1997; Sanders and Straub, 2002). Previous studies have also shown norepinephrine depletion in C57BL/6 mice increased Th1-associated cytokine responses to antigen-induced activation, indicating catecholamine signaling can influence naïve and Th1 cell cytokine production *in vivo* (Kruszewska et al., 1995). Furthermore, glucocorticoid activity has been shown to suppress the development of adaptive immunity by down-regulating the expression of MHC II and associated co-stimulatory molecules (Pan et al., 2001). Our results support and extend these findings by demonstrating muted expression of CD86 and MHC II expression on APCs following injury when compared to control animals. Moreover, muted APC activation was associated with a selective impairment in virus-specific CD4⁺ T cell effector functions including proliferation and secretion of the antiviral cytokine IFN- γ . Although infection of injured mice resulted in reduced CD4⁺ T cell numbers and proliferation within the spleen, injured mice also showed increases in total APCs and CD8⁺ T cells. Thus, it is possible that these alterations contribute to changes in spleen weight following infection, as the percent enlargement was similar between injured and un-injured mice. Injury also negatively impacts the number of virus-specific CD4⁺ T cells within the livers of infected mice, thus migration of these cells from lymphatic tissue may also be affected following SCI. Furthermore, expression of IFN- γ is associated with control of MHV replication and this is likely a contributing cause of elevated viral titers within the livers of infected T3-injured mice (Schijns et al., 1998). Therefore, diminished APC activity and Th1-associated responses observed following infection of T3-injured mice may be consequences of SNS and HPA-axis hyperactivity and this is a focus of on-going work.

It is likely that similar impairment of immune responses to infection seen in T3-injured mice may occur in mice with T9-injury, as increased sensitivity to viral infection was seen in both injury models. Studies of subjects with tetraplegia and paraplegia, who had been injured for at least 7 years, had significantly reduced T lymphocyte effector function compared to control subjects, and this deficit was similar in both injury groups studied (Iversen et al., 2000). Similarly, severe SCI at high or low thoracic levels in rats resulted in comparable deficits in ConA stimulated proliferation of T splenocytes when compared to control rats at various times post-injury (Ibarra et al., 2007). These findings suggest other immune-

regulating factors may contribute to diminished lymphocyte effector function following SCI in our infection model, as well as other experimental and clinical models. Indeed, immune responses within the spleen can be regulated by direct neurotransmitter interaction and by humoral influences of SNS and HPA-axis activity. Although SCI at T3 and not T9 disrupts descending outflow of SNS activity to the spleen, injury at both levels may still affect adrenal medulla sympathetic regulation. Thus, endocrine-mediated signaling to the spleen via the blood may contribute to SCI-induced immune suppression following MHV infection. If for instance, SNS activity becomes tonically active below the level of injury due to loss of supraspinal inhibitory regulation, then stimulus induced by infection, may cause both hyper-activation at nerve terminals and catecholamine release. Similar deregulation has been observed when infection exacerbated stroke-induced immune depression and was linked to increased SNS activity and greater impairment of CD4⁺ T cell activity compared to uninfected subjects with stroke-CIDS (Klehmet et al., 2009). Therefore, the contribution of sympathetic innervation of the spleen to the development anti-viral immune responses in our SCI-infection model may be better addressed in combinatory studies involving splenic nerve cut and SCI at a level low enough to preserve adrenal medulla SNS activity.

Our findings highlight that SCI negatively impacts immune-mediated control of an invading pathogen. Specifically, these data provide evidence that APC activation within the spleen is decreased which impairs the generation of sufficient numbers of virus-specific CD4⁺ T cells required for control and elimination of MHV. Future studies will focus on (i) how SCI induces changes in autonomic and neuroendocrine regulation of immunity over time, (ii) how these changes are compounded following experimental viral infection, and (iii) how SCI may alter immunological memory host defense mechanisms. Here we have observed SCI-induced immune suppression following primary infection. However, people with SCI experience recurrent infection, especially of the bladder and respiratory tract, suggesting deficits in secondary-memory responses that may contribute to immune suppression over time (Cardenas et al., 2004). Indeed, studies focused to elucidate immunological memory following SCI may lead to important insight into how injury results in potentially life-long immune deficiencies and lead to changes in vaccine treatment and boost regime for those with SCI. Therefore, understanding both primary and secondary-memory immune changes following SCI is valuable for the identification of possible novel therapeutic approaches to amplify immune responses and provide enhanced protection against infectious diseases.

Acknowledgments

The authors thank the Reeve-Irvine Research Center and the Roman Reed Spinal Cord Research Program for facility and personnel support. Funding was provided by the Craig H. Neilsen Foundation and RR09-CY2009 (Roman Reed Spinal Cord Injury Research Program of the State of California) to T.E.L. K.S.H. was supported, in part, by NIH T32 NS045540-05 training grant.

Abbreviations

SCI	spinal cord injury
Th2	Type-2T helper cell
i.p.	intraperitoneal

APCs	antigen presenting cells
SNS	sympathetic nervous system
HPA-axis	hypothalamic-pituitary-adrenal axis
CIDS	CNS immune deficiency syndrome
CNS	central nervous system
MHV	mouse hepatitis virus
Th1	Type-1T helper cell
p.i.	post-infection
AR	adrenergic receptor

References

- Bellinger DL, Felten SY, Lorton D, Feltenm DL. Innervation of lymphoid organs and neurotransmitter–lymphocyte interaction. *Immunol. Nerv. Syst.* 1979;226–329.
- Bergmann CC, Yao Q, Lin M, Stohlman SA. The JHM strain of mouse hepatitis virus induces a spike protein-specific Db-restricted cytotoxic T cell response. *J. Gen. Virol.* 1996; 77(Pt 2):315–325. [PubMed: 8627236]
- Campagnolo DI, Bartlett JA, Keller SE, Sanchez W, Oza R. Impaired phagocytosis of *Staphylococcus aureus* in complete tetraplegics. *Am. J. Phys. Med. Rehabil.* 1997; 76:276–280. [PubMed: 9267186]
- Campagnolo DI, Dixon D, Schwartz J, Bartlett JA, Keller SE. Altered innate immunity following spinal cord injury. *Spinal Cord.* 2008; 46:477–481. [PubMed: 18268516]
- Cano G, Sved AF, Rinaman L, Rabin BS, Card JP. Characterization of the central nervous system innervation of the rat spleen using viral transneuronal tracing. *J. Comp. Neurol.* 2001; 439:1–18. [PubMed: 11579378]
- Cardenas DD, Hoffman JM, Kirshblum S, McKinley W. Etiology and incidence of rehospitalization after traumatic spinal cord injury: a multicenter analysis. *Arch. Phys. Med. Rehabil.* 2004; 85:1757–1763. [PubMed: 15520970]
- Castro RF, Perlman S. CD8+ T-cell epitopes within the surface glycoprotein of a neurotropic coronavirus and correlation with pathogenicity. *J. Virol.* 1995; 69:8127–8131. [PubMed: 7494335]
- Cruse JM, Keith JC, Bryant ML Jr, Lewis RE Jr. Immune system-neuroendocrine dysregulation in spinal cord injury. *Immunol. Res.* 1996; 15:306–314. [PubMed: 8988397]
- Cruse JM, Lewis RE, Dilioglou S, Roe DL, Wallace WF, Chen RS. Review of immune function, healing of pressure ulcers, and nutritional status in patients with spinal cord injury. *J. Spinal Cord Med.* 2000a; 23:129–135. [PubMed: 10914354]
- Cruse JM, Lewis RE, Roe DL, Dilioglou S, Blaine MC, Wallace WF, Chen RS. Facilitation of immune function, healing of pressure ulcers, and nutritional status in spinal cord injury patients. *Exp. Mol. Pathol.* 2000b; 68:38–54. [PubMed: 10640453]
- Downing JE, Miyan JA. Neural immunoregulation: emerging roles for nerves in immune homeostasis and disease. *Immunol. Today.* 2000; 21:281–289. [PubMed: 10825740]
- Eriksson KK, Cervantes-Barragan L, Ludewig B, Thiel V. Mouse hepatitis virus liver pathology is dependent on ADP-ribose-1st-phosphatase, a viral function conserved in the alpha-like supergroup. *J. Virol.* 2008; 82:12325–12334. [PubMed: 18922871]
- Held KS, Glass WG, Orlovsky YI, Shamberger KA, Petley TD, Branigan PJ, Carton JM, Beck HS, Cunningham MR, Benson JM, Lane TE. Generation of a protective T-cell response following coronavirus infection of the central nervous system is not dependent on IL-12/23 signaling. *Viral Immunol.* 2008; 21:173–188. [PubMed: 18570589]

- Hirano N, Murakami T, Fujiwara K, Matsumoto M. Utility of mouse cell line DBT for propagation and assay of mouse hepatitis virus. *Jpn J. Exp. Med.* 1978; 48:71–75. [PubMed: 209230]
- Ibarra A, Jimenez A, Cortes C, Correa D. Influence of the intensity, level and phase of spinal cord injury on the proliferation of T cells and T-cell-dependent antibody reactions in rats. *Spinal Cord.* 2007; 45:380–386. [PubMed: 16955070]
- Iversen PO, Hjeltnes N, Holm B, Flatebo T, Strom-Gundersen I, Ronning W, Stanghelle J, Benestad HB. Depressed immunity and impaired proliferation of hematopoietic progenitor cells in patients with complete spinal cord injury. *Blood.* 2000; 96:2081–2083. [PubMed: 10979951]
- Klehmet J, Harms H, Richter M, Prass K, Volk HD, Dirnagl U, Meisel A, Meisel C. Stroke-induced immunodepression and post-stroke infections: lessons from the preventive antibacterial therapy in stroke trial. *Neuroscience.* 2009; 158:1184–1193. [PubMed: 18722511]
- Kruszewska B, Felten SY, Moynihan JA. Alterations in cytokine and antibody production following chemical sympathectomy in two strains of mice. *J. Immunol.* 1995; 155:4613–4620. [PubMed: 7594460]
- Lane TE, Liu MT, Chen BP, Asensio VC, Samawi RM, Paoletti AD, Campbell IL, Kunkel SL, Fox HS, Buchmeier MJ. A central role for CD4(+) T cells and RANTES in virus-induced central nervous system inflammation and demyelination. *J. Virol.* 2000; 74:1415–1424. [PubMed: 10627552]
- Lorton D, Lubahn C, Lindquist CA, Schaller J, Washington C, Bellinger DL. Changes in the density and distribution of sympathetic nerves in spleens from Lewis rats with adjuvant-induced arthritis suggest that an injury and sprouting response occurs. *J. Comp. Neurol.* 2005; 489:260–273. [PubMed: 15984001]
- Lucin KM, Sanders VM, Jones TB, Malarkey WB, Popovich PG. Impaired antibody synthesis after spinal cord injury is level dependent and is due to sympathetic nervous system dysregulation. *Exp. Neurol.* 2007; 207:75–84. [PubMed: 17597612]
- Lucin KM, Sanders VM, Popovich PG. Stress hormones collaborate to induce lymphocyte apoptosis after high level spinal cord injury. *J. Neurochem.* 2009; 110:1409–1421. [PubMed: 19545280]
- MacNeil, B; Nance, DM. Skin inflammation and immunity after spinal cord injury. In: Berczi, I.; Szentivanyi, A., editors. *Neuroimmune Biology, New Foundation of Biology.* Amsterdam, The Netherlands: Elsevier Science B.V.; 2001. p. 455–469.
- Matthews AE, Weiss SR, Shlomchik MJ, Hannum LG, Gombold JL, Paterson Y. Antibody is required for clearance of infectious murine hepatitis virus A59 from the central nervous system, but not the liver. *J. Immunol.* 2001; 167:5254–5263. [PubMed: 11673540]
- Meisel C, Schwab JM, Prass K, Meisel A, Dirnagl U. Central nervous system injury-induced immune deficiency syndrome. *Nat. Rev. Neurosci.* 2005; 6:775–786. [PubMed: 16163382]
- Mignini F, Streccioni V, Amenta F. Autonomic innervation of immune organs and neuroimmune modulation. *Auton. Autacoid Pharmacol.* 2003; 23:1–25. [PubMed: 14565534]
- Muse M, Kane JA, Carr DJ, Farber JM, Lane TE. Insertion of the CXC chemokine ligand 9 (CXCL9) into the mouse hepatitis virus genome results in protection from viral-induced encephalitis and hepatitis. *Virology.* 2008; 382:132–144. [PubMed: 18973912]
- Navas S, Seo SH, Chua MM, Das Sarma J, Lavi E, Hingley ST, Weiss SR. Murine coronavirus spike protein determines the ability of the virus to replicate in the liver and cause hepatitis. *J. Virol.* 2001; 75:2452–2457. [PubMed: 11160748]
- Pan J, Ju D, Wang Q, Zhang M, Xia D, Zhang L, Yu H, Cao X. Dexamethasone inhibits the antigen presentation of dendritic cells in MHC class II pathway. *Immunol. Lett.* 2001; 76:153–161. [PubMed: 11306142]
- Riegger T, Conrad S, Liu K, Schluesener HJ, Adibzahdeh M, Schwab JM. Spinal cord injury-induced immune depression syndrome (SCI-IDS). *Eur. J. Neurosci.* 2007; 25:1743–1747. [PubMed: 17432962]
- Sanders VM, Straub RH. Norepinephrine, the beta-adrenergic receptor, and immunity. *Brain Behav. Immun.* 2002; 16:290–332. [PubMed: 12096881]
- Sanders VM, Baker RA, Ramer-Quinn DS, Kasprovicz DJ, Fuchs BA, Street NE. Differential expression of the beta2-adrenergic receptor by Th1 and Th2 clones: implications for cytokine production and B cell help. *J. Immunol.* 1997; 158:4200–4210. [PubMed: 9126981]

- Schijns VE, Haagmans BL, Wierda CM, Kruithof B, Heijnen IA, Alber G, Horzinek MC. Mice lacking IL-12 develop polarized Th1 cells during viral infection. *J. Immunol.* 1998; 160:3958–3964. [PubMed: 9558103]
- Schmid FA, Pena RC, Robinson W, Tarnowski GS. Toxicity of intraperitoneal injections of 7, 12-dimethylbenz[a]anthracene in inbred mice. *Cancer Res.* 1967; 27:558–562. [PubMed: 6021513]
- Soden RJ, Walsh J, Middleton JW, Craven ML, Rutkowski SB, Yeo JD. Causes of death after spinal cord injury. *Spinal Cord.* 2000; 38:604–610. [PubMed: 11093321]
- Stiles LN, Hardison JL, Schaumburg CS, Whitman LM, Lane TE. T cell antiviral effector function is not dependent on CXCL10 following murine coronavirus infection. *J. Immunol.* 2006; 177:8372–8380. [PubMed: 17142734]
- Teasell RW, Arnold JM, Krassioukov A, Delaney GA. Cardiovascular consequences of loss of supraspinal control of the sympathetic nervous system after spinal cord injury. *Arch. Phys. Med. Rehabil.* 2000; 81:506–516. [PubMed: 10768544]
- Trifilo MJ, Montalto-Morrison C, Stiles LN, Hurst KR, Hardison JL, Manning JE, Masters PS, Lane TE. CXC chemokine ligand 10 controls viral infection in the central nervous system: evidence for a role in innate immune response through recruitment and activation of natural killer cells. *J. Virol.* 2004; 78:585–594. [PubMed: 14694090]
- Walsh KB, Edwards RA, Romero KM, Kotlajich MV, Stohlman SA, Lane TE. Expression of CXC chemokine ligand 10 from the mouse hepatitis virus genome results in protection from viral-induced neurological and liver disease. *J. Immunol.* 2007; 179:1155–1165. [PubMed: 17617609]
- Walsh KB, Lodoen MB, Edwards RA, Lanier LL, Lane TE. Evidence for differential roles for NKG2D receptor signaling in innate host defense against coronavirus-induced neurological and liver disease. *J. Virol.* 2008; 82:3021–3030. [PubMed: 18094157]
- Wijburg OL, Heemskerk MH, Sanders A, Boog CJ, Van Rooijen N. Role of virus-specific CD4+ cytotoxic T cells in recovery from mouse hepatitis virus infection. *Immunology.* 1996; 87:34–41. [PubMed: 8666433]
- Xue S, Jaszewski A, Perlman S. Identification of a CD4+ T cell epitope within the M protein of a neurotropic coronavirus. *Virology.* 1995; 208:173–179. [PubMed: 11831697]

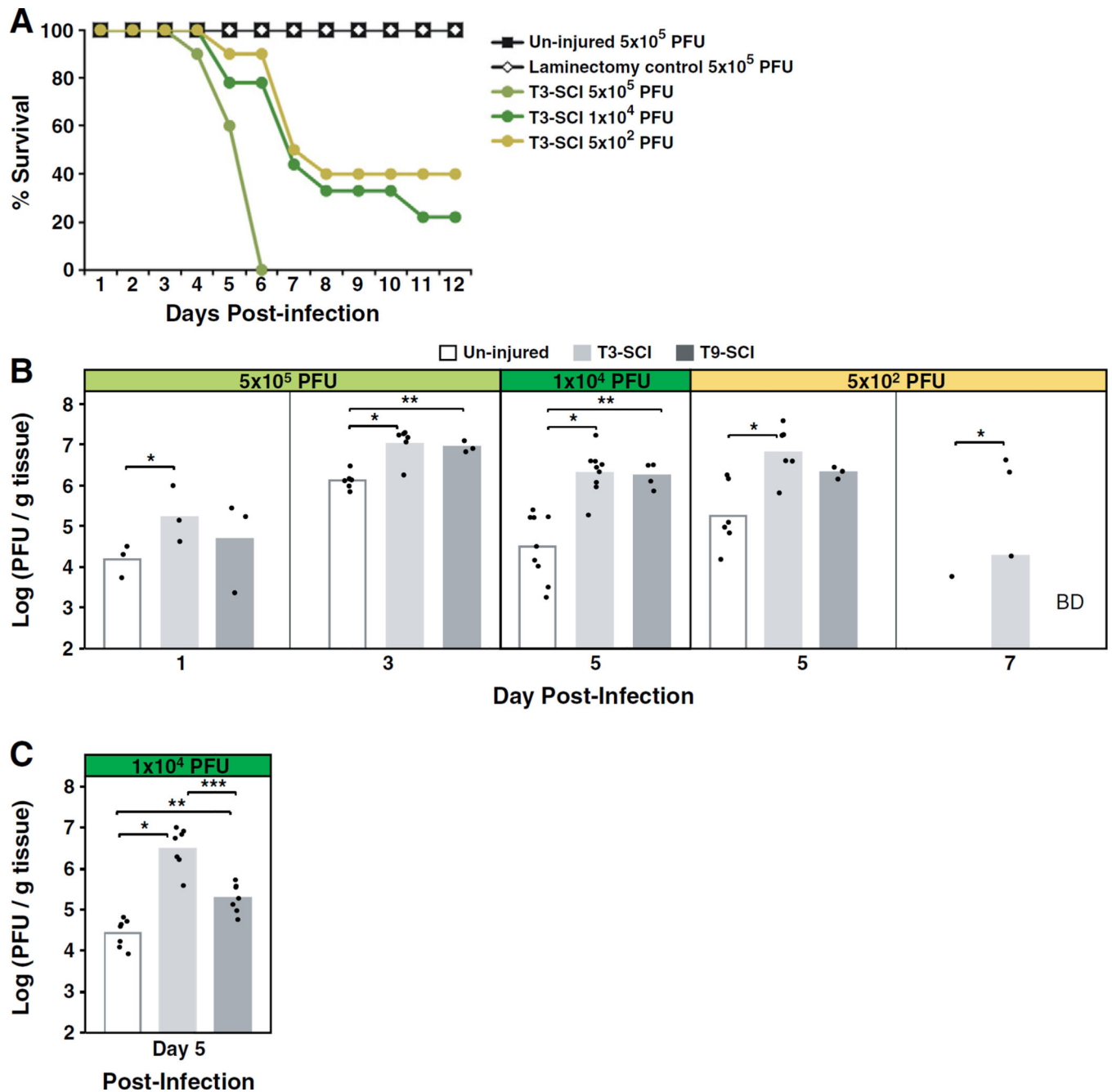


Fig. 1. Spinal cord injured mice exhibit increased mortality and higher viral titer following viral infection compared to un-injured infected mice. At 1 week post-SCI, mice were infected with increasing dosages of MHV (5×10^2 – 5×10^5 PFU) and mortality recorded. A) The survival of T3-injured mice following 5×10^5 PFU infection resulted in mortality, yet 100% survival was observed in un-injured mice and laminectomy surgery-control mice. Survival of T3-injured mice was prolonged following infection at lower dosages. Viral titers were recorded following infection at 1 week (B) and 4 weeks (C) post-SCI in T3- and T9-injured mice. Injured mice showed higher viral titers compared to un-injured mice at all infection

dosages, independent of infection time post-SCI. Survival studies began with 10–8 mice in each infection group. Viral titers are presented as logarithmic means of PFU per gram of liver, as shown in columns in B and C bar graphs, with each data point representing one mouse. The limit of detection was ~200 PFU/g liver; BD=below level of detection. Significant differences between T3-injured and un-injured controls (*p < 0.05), T9-injured and un-injured controls (**p < 0.02), and T3-injured and T9-injured (***p < 0.003) groups are shown in B and C.

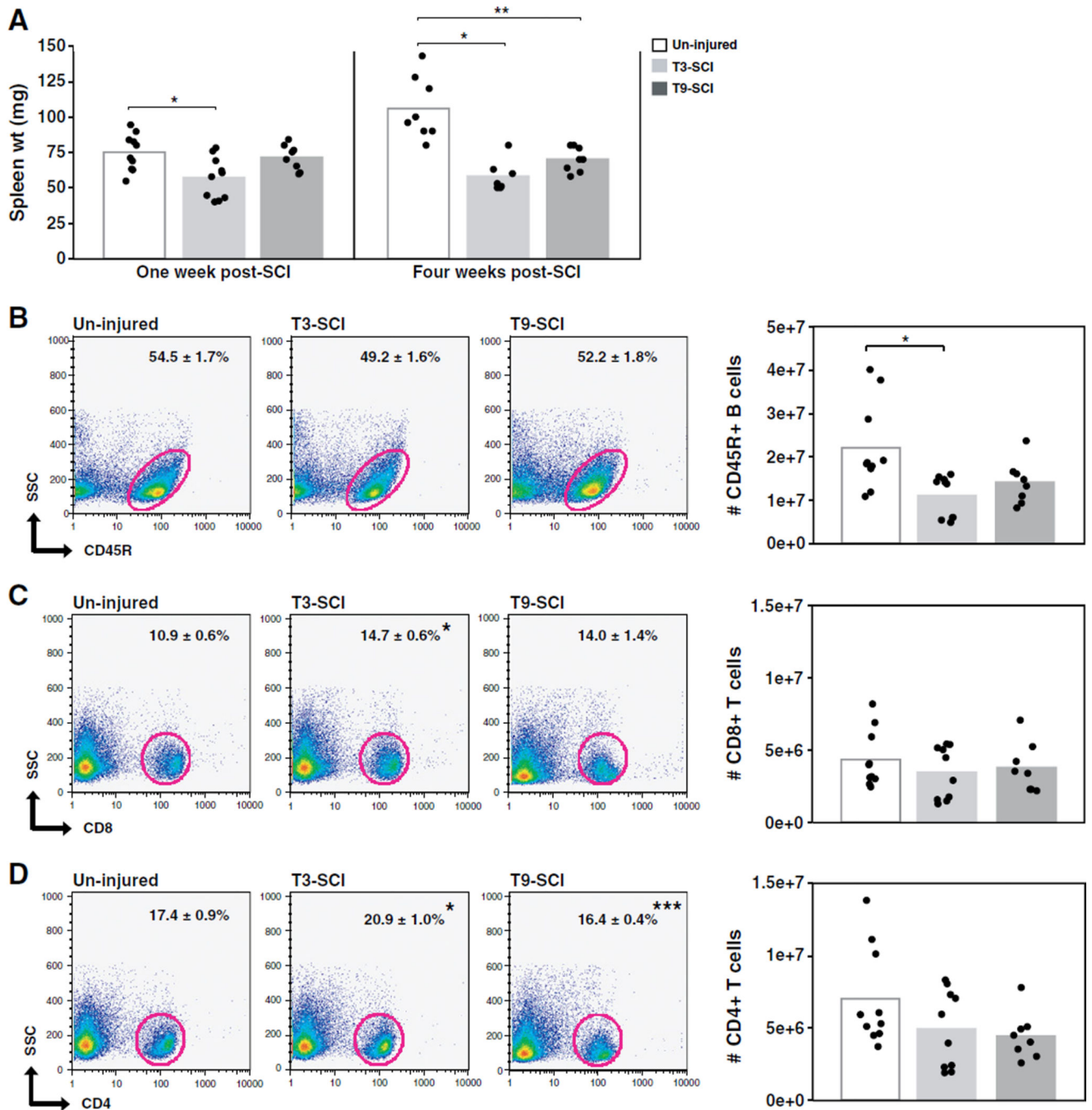
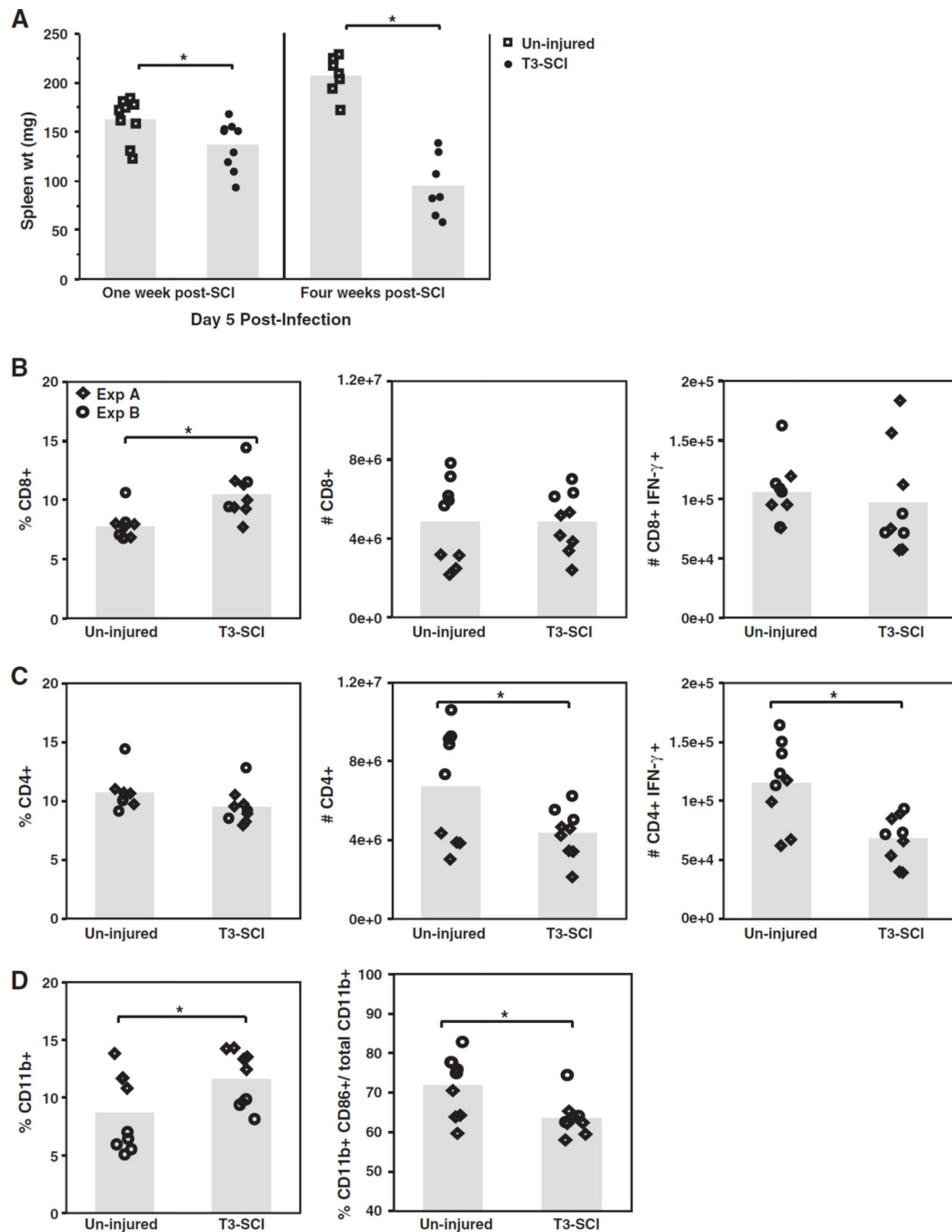


Fig. 2. T3-injured mice have reduced spleen size and decreased number of B lymphocytes prior to MHV infection. Spleen weight and lymphocyte populations were examined in injured and un-injured mice prior to infection. A) T3-injured and not T9-injured mice showed significant reduction in spleen weight compared to un-injured controls at 1 week post-SCI (*p = 0.004). The average mean weight of injured mice did not increase over time like un-injured mice, thus both T3-injured (*p = 0.001) and T9-injured (**p = 0.001) mice had significantly reduced spleen weights at 4 weeks post-SCI compared to un-injured controls. Following 1

week post-SCI, spleens were collected and processed for flow cytometric analysis of B and T lymphocytes. B–D) Representative dot plots show the frequency (mean \pm SEM) positive cells within gated population, with the corresponding number in adjacent bar graphs. The frequencies of CD45R⁺ B cells in T9-injured and un-injured mice were similar (B, dot plots). However the frequency in T3-injured mice was reduced (B, dot plots), and there was a significant decrease in the number of B cells compared to un-injured controls (*p = 0.002) (B, graph). The number of B cells in T9-injured mice was reduced compared to un-injured control, but was not significantly different (B, graph). Injured mice showed similar increases in the frequency of CD8⁺ T cells, however only T3-injured mice had significant increase compared to un-injured controls (*p = 0.004) (C, dot plots). Comparison of the numbers of CD8⁺ T cells between all experimental groups revealed no significant differences (C, graph). There was no significant difference in the frequency of CD4⁺ T cells from T9-injured and un-injured mice (D, dot plots). However, T3-injured mice showed significantly increased frequency of CD4⁺ T cells compared to un-injured mice (*p = 0.006) and T9-injured mice (***p = 0.001) (D, dot plots). Although injured mice show reduced numbers of CD4⁺ T cells compared to un-injured mice, comparison between all experimental groups revealed no significant differences (D, graph). Each data point represents one mouse, and the group mean is presented as column in bar graphs.

**Fig. 3.**

Spleen size and the generation of an adaptive immune response are reduced following infection of T3-injured mice. Spleen size increases following infection, thus on day 5 p.i. with 1×10^4 PFU MHV spleen weight and cellular composition were assessed. A) Following infection at 1 week and 4 weeks post-SCI, T3-injured mice showed significantly reduced spleen weight compared to un-injured mice (* $p < 0.03$). B–D) At 1 week post-SCI, T3-SCI mice were infected with 1×10^4 PFU and the generation of an adaptive immune response in the spleen evaluated on day 5 p.i. using flow cytometric analysis. Virus-specific

T cells were determined by ex vivo stimulation with CD4 Ag-specific peptide (epitope M133–147), CD8 Ag-specific peptide (epitope S598–605), or non-specific OVA control peptide, prior to flow cytometric assessment. T3-injured mice showed significant increase (*p = 0.002) in the frequency of CD8⁺ T cells compared to un-injured mice (B, first panel), however there was no difference in the number of total CD8⁺ T cells nor the number of virus-specific CD8⁺ IFN- γ ⁺ T cells (B, second and right-hand panels). The frequency of CD4⁺ T lymphocytes was similar between infected T3-injured and un-injured mice (C, first panel), however the numbers of total CD4⁺ and virus-specific CD4⁺ IFN- γ ⁺ T cells were significantly reduced in injured mice (*p = 0.04) (C, second and right-hand panels). The frequency of CD11b⁺ macrophages was significantly increased in T3-injured mice (*p = 0.04) (D, first panel), however the frequency of CD86⁺ activated CD11b⁺ macrophages within the total macrophage population was significantly decreased compared to un-injured mice (*p = 0.01) (D, second panel). The mean number of cells is presented in bar graphs, with each data point representing one mouse from two separate experiments.

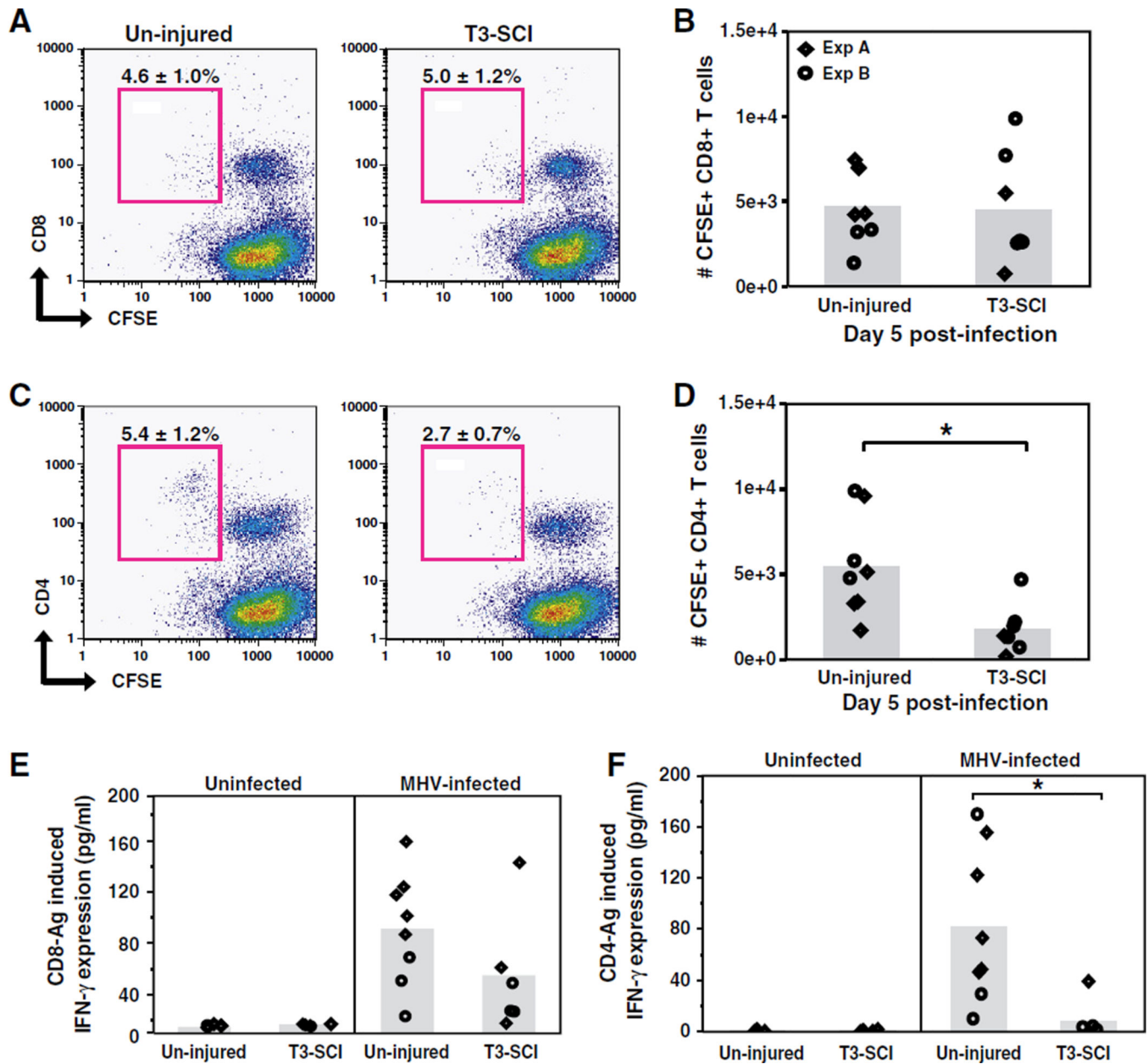


Fig. 4. SCI suppresses CD4⁺ T cell effector functions following infection. T3-injured mice were infected with 1×10^4 PFU MHV 1 week post-injury, and splenocytes harvested at day 5 p.i. Cells were stimulated with CD4 Ag-specific peptide (epitope M133–147), CD8 Ag-specific peptide (epitope S598–605), or non-specific OVA control peptide to determine proliferation and IFN- γ production. A) The frequency of proliferating CFSE-labeled CD8⁺ responding to CD8 Ag-specific peptide was similar in T3-injured and un-injured mice. B) There was no difference in proliferation of Ag-specific CD8⁺ T cells, indicated by similar total number of CFSE⁺ CD8⁺ T cells between injured and un-injured mice. C) T3-injured mice showed a decrease in the frequency of proliferating CFSE-labeled CD4⁺ responding to CD4 Ag-specific peptide compared un-injured mice, but the difference was not significant. D) T3-

injured mice, however, showed a significant decrease in proliferation of Ag-specific CD4⁺ T cells (*p = 0.007), compared to un-injured mice, as indicated by the total number of CFSE⁺ CD4⁺ T cells. E) ELISA assay revealed splenocytes from infected mice that were stimulated with CD8 Ag-specific peptide induced similar IFN- γ protein expression between T3-injured and un-injured mice, while (F) CD4 Ag-specific peptide stimulation resulted in significantly reduced IFN- γ expression in T3-injured mice compared to un-injured mice (*p = 0.001). CD8 or CD4-Ag stimulation of splenocytes from uninfected mice induced very low, yet comparable levels of IFN- γ between T3-injured and un-injured mice (E and F). Representative dot plots are shown in A and C, and the frequency (mean \pm SEM) of dual-positive cells indicated above the gate. The corresponding number of proliferating CFSE-labeled virus-specific T cells shown in B and D, is relative to the number of CD8⁺ and CD4⁺ virus-specific T cells, respectively. Cytokine expression in E and F is reported as fold-change to OVA control peptide stimulation. The mean number of cells is presented in bar graphs, with each data point representing one mouse from two separate experiments.

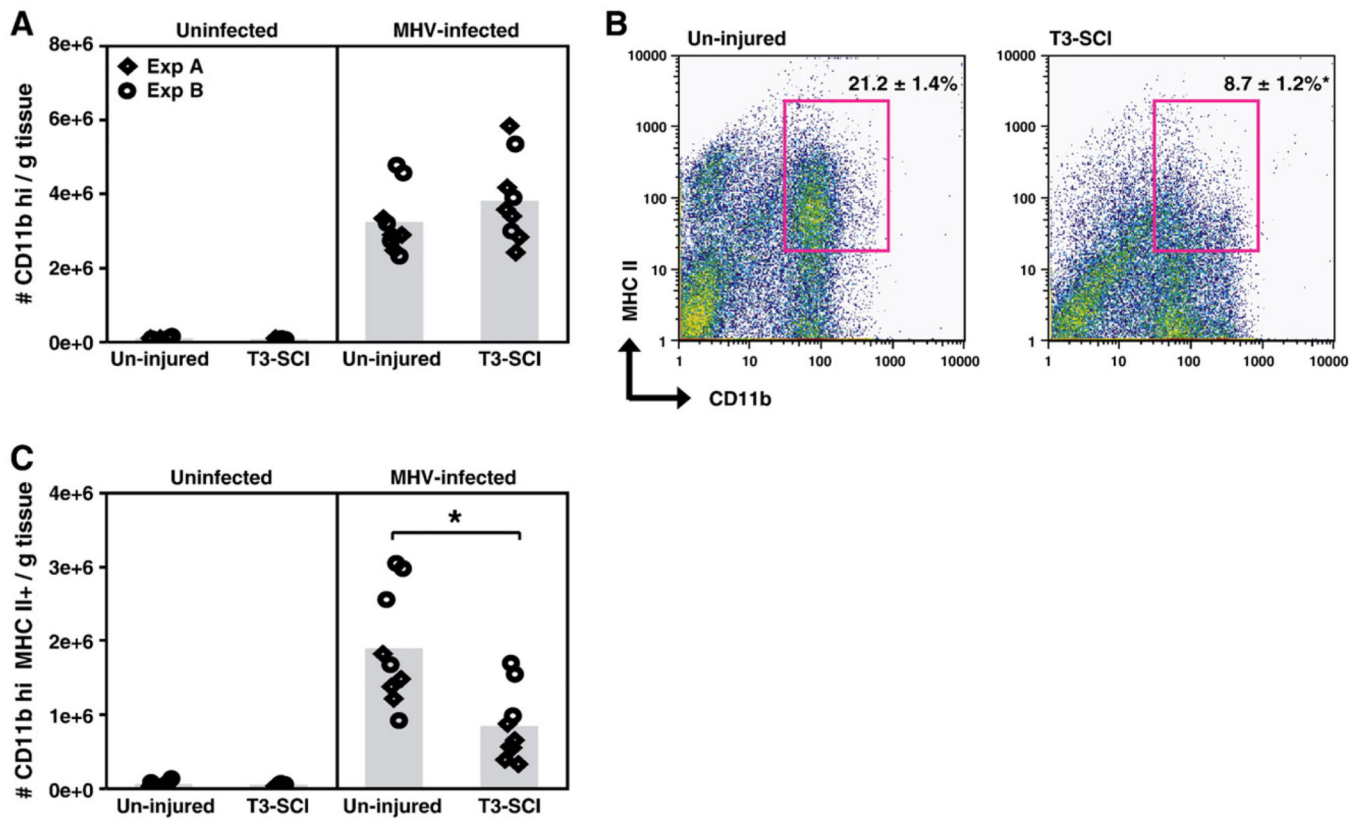


Fig. 5. Infection of T3-injured mice results in decreased activated macrophages in the liver. 1 week following SCI, mice were infected with 1×10^4 PFU MHV and livers collected and processed for flow cytometric analysis of activated macrophages. A) At day 5 p.i., the numbers of macrophages in the liver were similar between T3-injured and un-injured mice. However, the frequencies of gated MHC II⁺ CD11b^{hi} activated macrophages (B) and the corresponding numbers (C) were significantly reduced in T3-injured mice, compared to uninjured mice following infection (* $p < 0.003$). Prior to infection, the total numbers of CD11b^{hi} macrophages and CD11b^{hi} MHC II⁺ activated macrophages were minimal, yet similar between T3-injured and un-injured uninfected mice (A and C). The mean number of cells is presented in bar graphs (A and C) with each data point representing one mouse from two separate experiments. Representative dot plots from infected mice are shown in B, and the frequency (mean \pm SEM) of dual-positive cells is indicated in the upper right quadrant.

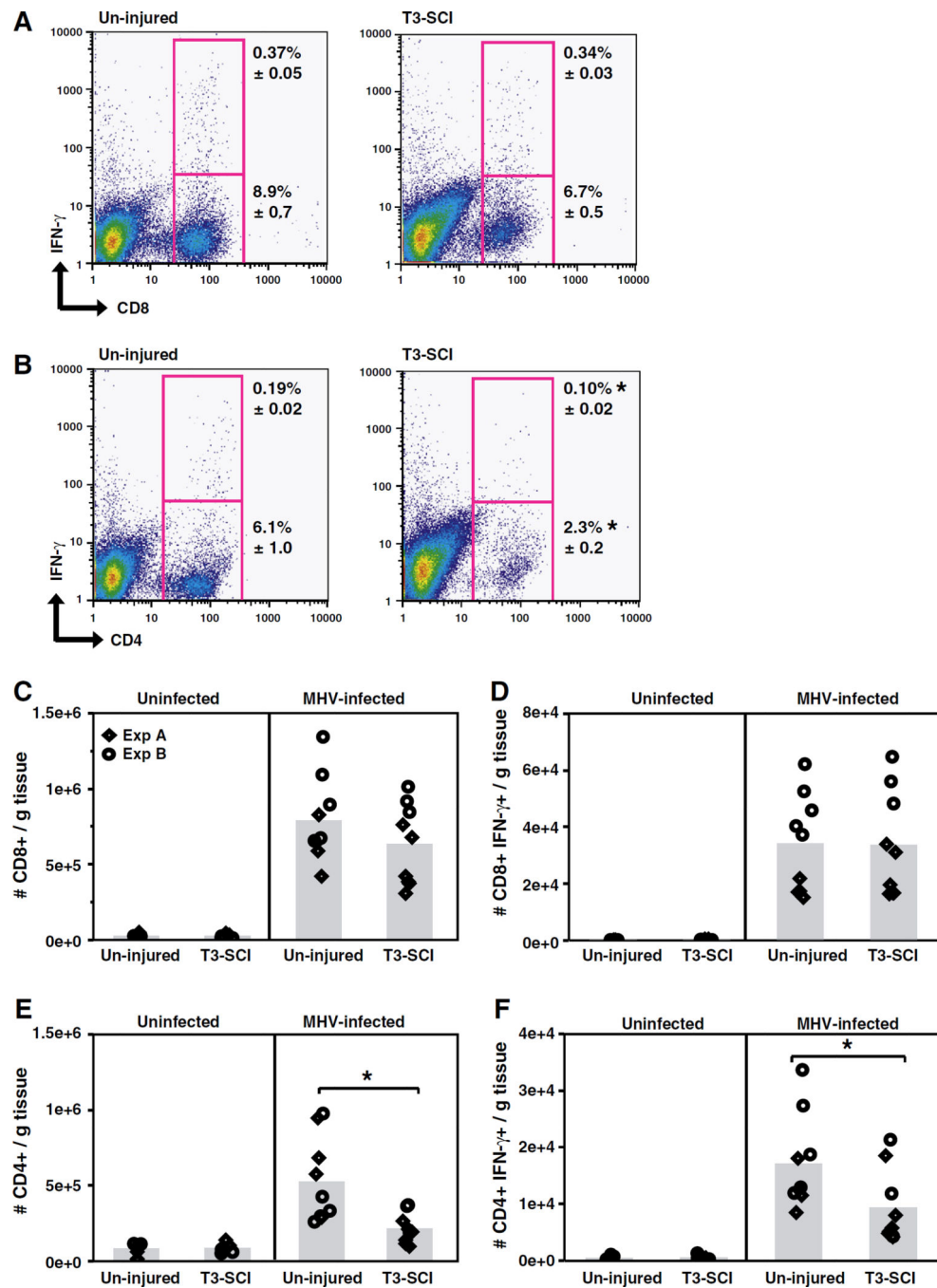


Fig. 6. MHV-specific CD4⁺ T cell infiltration to the liver is altered following SCI. 1 week following SCI, mice were infected with 1×10^4 PFU MHV, and livers collected at day 5 p.i. Tissues were processed for ex vivo peptide stimulation and subsequent flow cytometric analysis to determine the infiltration of adaptive T lymphocytes to the liver. Following MHV infection, the frequency (A, lower gate) and numbers (C) of CD8⁺ T cells in the liver were comparable between T3-injured and un-injured mice. T3-injured mice showed significant decrease in frequency (B, lower gate) and numbers (E) of CD4⁺ T cells in the liver compared to un-

injured mice (*p = 0.006). In addition, there was significant decrease in the infiltration of Ag-specific CD4⁺ T cells, indicated by decreased frequency (B, upper gate) and total numbers (F) of virus-specific CD4⁺ T cells expressing IFN- γ in T3-injured mice compared to un-injured mice, as determined by intracellular cytokine staining following stimulation with CD4 epitope M133–147 (*p = 0.01). There were similar frequencies (A, upper gate) and numbers (D) of virus-specific CD8⁺ IFN- γ ⁺ T cells between T3-injured and un-injured mice as determined by intracellular cytokine staining following stimulation with CD8 epitope S598–605. Prior to infection, the total numbers of assessed T lymphocyte populations were minimal, yet similar between T3-injured and un-injured mice (C–F). Representative dot plots are shown in A and B, with the frequency (mean \pm SEM) of CD8 and CD4 single-positive cells, indicated in lower gate, and the corresponding number in C and E bar graphs. Representative dot plots also show the frequency (mean \pm SEM) of CD8/IFN- γ or CD4/IFN- γ dual-positive cells, indicated in upper gate, and the corresponding number in D and F bar graphs. The mean number of cells is presented in bar graphs (C–F) with each data point representing one mouse from two separate experiments.